Journal of the Nigerian Association of Mathematical Physics
Volume 29, (*March, 2015*), pp 111 – 124

Unsteady Radiative Hydromagnetic Internal Heat Generating Fluid Flow Through a Porous Channel of a Two-Step Exothermic Chemical Reaction

[1]Kareem R. A. and [2]Gbadeyan J. A.

[1]Department of Mathematics, Lagos State Polytechnic, Ikorodu, Nigeria
[2]Department of Mathematics, University of Ilorin, Ilorin, Nigeria.

Abstract

In this study, the problem of an unsteady reactive viscous combustible fluid flowing through a porous channel with radiation under different chemical kinetics namely: Sensitized, Arrhenius and Bimolecular of a two-step exothermic chemical reaction is investigated. The fluid is acted upon by the pressure gradient along the axis of the channel in the presence of uniform magnetic field with isothermal wall temperature. Solutions of the nonlinear dimensionless equations governing the fluid flow were obtained using a combined Laplace Differential Transform Method (LDTM). The influence of the various fluid parameters associated to the problem on velocity and temperature are discussed and presented through graphs.

Keywords: Reactive fluid, Unsteady, Exothermic reaction, Sensitized, Arrhenius, Bimolecular and Laplace Differential Transform

Nomenclature

$\bar{u}$	Dimensional axial velocity,	u	Non-dimensional axial velocity,
$\bar{P}$	Dimensional modified pressure,	P	Non-dimensional modified pressure,
±	Electrical conductivity,	B_0	magnetic field strength,
$\bar{T}$	Dimensional fluid temperature,	T	Non-dimensional fluid temperature,
T_0	Initial temperature,	T_w	Wall temperature,
$\bar{t}$	Time,	k	thermal conductivity coefficient,
K	Boltzmann's constant,	l	Planck's number,
³	Vibration frequency,	R	Universal gas constant,
C_p	Specific heat at constant pressure,	r	activation energy ratio parameter,
∘	Fluid density,	a	Frank-Kamenetskii parameter,
£	Activation energy parameter,		Heat source parameter,
¥	Two-step reaction parameter,	m	Numerical exponent,
Q_1	First step heat of reaction,	Q_2	Second step heat of reaction,
C_1	First step initial concentration,	C_2	second step initial concentration,
A_1	First step reaction rate,	A_2	Second step reaction rate,
E_1	First step activation energy,	E_2	second step activation energy,
Q_0	Dimensional heat generation coefficient,	Br	Brinkman number,
H	Hartman number,	G	Pressure gradient,
Pr	Prandtl number.		

Corresponding author: Kareem R. A, E-mail: , Tel.: +2348032018520

1.0 Introduction

The transient flow of electrically conducting viscous fluid has been investigated extensively due to its applications in magnetohydrodynamics (MHD) pumps, accelerators, aerodynamics, petroleum industry and fluid droplets-sprays. Spontaneous explosion due to internal heating in combustible materials such as industrial waste fuel, coal and wool waste can be described by thermal explosion theory [1]. In fact, evaluation of the critical regimes thought of as regimes separating the region of explosive and nonexplosive ways of chemical reactions is the main mathematical theory of explosion [2-4]. The mathematical formulation of the problem was first initiated by Frank-Kamenestkii.

The study of reactive magnetohydrodynamics flow has applications in industries and engineering. Also in polymer extrusion, nuclear reactor design, geophysics and energy storage systems. In the light of these applications, Makinde [5] presented thermal stability of a reactive viscous flow through a porous saturated channel with convective boundary conditions. Makinde and Anwar Beg [6] considered the inherent irreversibility in a reactive hydromagnetic channel flow. Extensively, Hassan [7] investigated on single step exothermic chemical reaction and reported the influence of Sensitized, Arrhenius and Bimolecular chemical kinetics. More so, Makinde et al.[8] presented the thermal stability of a two-step exothermic chemical reaction in a slab and reported the diffusion of reactant and the variable pre-exponential factor for both transient and steady state.

The study of fluid flow through a porous medium has received considerable attentions as a result of its applications in soil mechanisms, underground water hydrology, irrigation, agricultural ceramics engineering, chemical engineering and petroleum engineering.In view of these applications, effects of radiation on natural convection MHD flow in a porous channel filled with a porous medium were investigated by [9,10]. Hayat et al. [11] studied the thermal radiation in MHD channel flow with heat and mass transfer taking into account the simultaneous effects on heat and mass transfer on the MHD three dimensional channel flow of viscous fluid in the presence of thermal radiation. Analysis of the effects of hall current thermal radiation and first-order chemical reaction on the oscillatory convective flow and mass transfer with suction injection in a rotating vertical porous channel was reported by [12,13].

Bakr [14] revealed the chemical reaction effects on unsteady MHD oscillatory slip flow in an optically thin temperature-dependent heat source. Singh [15] studied an oscillatory mixed convection of an electrically conducting viscous incompressible flow in a vertical channel in the presence of heat radiation.Keeping the above studies in view, we present unsteady radiative hydromagnetic internal heat generating fluid flow through a porous channel of a two-step exothermic chemical reaction. A combined Laplace Differential Transform Method (LDTM) is used to obtain solutions of the resulting governing equations of the flow problem. The effects of pertinent parameters on fluid flow and heat transfer characteristics are discussed.

2.0 Mathematical Formulation

We consider the unsteady flow of an incompressible reactive hydromagnetic fluid of a two-step exothermic chemical reaction placed between two parallel plates induced by the combined action of applied axial pressure gradient and uniform motion of the upper plate. It is assumed that the flow is subjected to the influence of an externally applied magnetic field B_0 as shown in Figure 1.

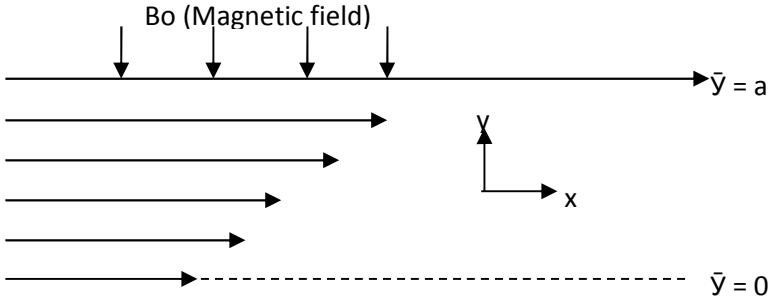

Figure 1: Geometry of the problem

The x-axis is taken along the center of the channel and the y-axis is taken normal to it. The governing equations for the momentum and energy equations can be written as:

$$\circ \frac{\partial \bar{u}}{\partial \bar{t}} = -\frac{\partial \bar{P}}{\partial \bar{x}} + \ll \frac{\partial^2 \bar{u}}{\partial \bar{y}^2} - \pm B_0^2 \bar{u} - \frac{\ll \bar{u}}{\overline{K_1}} \tag{1}$$

$$\circ C_p \frac{\partial \bar{T}}{\partial \bar{t}} = k \frac{\partial^2 \bar{T}}{\partial \bar{y}^2} - \frac{\partial \bar{q}}{\partial \bar{y}} + \ll \left(\frac{\partial \bar{u}}{\partial \bar{y}}\right)^2 + \pm B_0^2 \bar{u}^2 + Q_1 C_1 A_1 \left(\frac{K\bar{T}}{{}^3 l}\right)^m e^{\frac{E_1}{RT}} + Q_2 C_2 A_2 \left(\frac{K\bar{T}}{{}^3 l}\right)^m e^{\frac{E_2}{RT}} + Q_0 \left(\bar{T} - T_w\right) \tag{2}$$

Subject to relevant initial and boundary conditions

$$\bar{u}(\bar{y},0)=0,\bar{T}(\bar{y},0)=T_0,\bar{u}(0,\bar{t})=0,\bar{u}(a,\bar{t})=U,\bar{T}(0,\bar{t})=T_0,\bar{T}(a,\bar{t})=T_w \quad (3)$$

where the variables and the parameters are defined in the nomenclature. The numerical exponents $m \in \{-2,0,0.5\}$ represent chemical kinetics for Sensitized, Arrhenius and Bimolecular kinetics respectively.

The following dimensionless parameters are introduced

$$y=\frac{\bar{y}}{a},x=\frac{\bar{x}}{a},T=\frac{(\bar{T}-T_w)}{RT_w^2},G=-\frac{\partial P}{\partial x},P=\frac{a\bar{P}}{\ll U},H^2=\frac{\pm B_0^2 a^2}{\ll},\pounds=\frac{RT_w}{E_1},r=\frac{E_2}{E_1},$$

$$Br=\frac{\ll U^2 E_1}{KRT_w^2},\mathrm{a}=\frac{Q_1C_1A_1E_1a^2}{KRT_w^2}\left(\frac{R\bar{T}}{\mathrm{3}l}\right)^2 e^{\frac{1}{\pounds}},\quad =\frac{Q_0RT_w^2}{Q_1C_1A_1E_1}\left(\frac{\mathrm{3}l}{KT_w}\right)^m e^{-\frac{1}{\pounds}},¥=\frac{Q_2C_2A_2}{Q_1C_1A_1}e^{-\frac{r}{\pounds}}e^{\frac{1}{\pounds}}, \quad (4)$$

$$\mathrm{Pr}=\frac{\ll C_p}{k},t=\frac{\ll t}{\circ a^2},u=\frac{\bar{u}}{U},b=\frac{E_1(T_0-T_w)}{RT_w^2},K=\frac{\overline{K_1}}{a^2},R_1=\frac{ka_R}{4\pm T_\infty}$$

Following Rosseland approximation, Brewster [16], the radiative heat flux in the direction can be modeled as

$$q=-\frac{4\pm\partial T^4}{3a_R\partial\bar{y}} \quad (5)$$

where $\pm$ is the Stefan-Boltzmann constant and R_1 is the mean absorption coefficient. If the temperature difference within the flow are small such that T^4 can be expressed as a linear combination of the temperature, then the Taylor series T^4 for about T_∞, neglecting higher order terms, is

$$T^4=4T_\infty^3-3T_\infty^4 \quad (6)$$

Using the dimensionless parameters (4) into equations $(1)-(3)$, we obtain

$$\frac{\partial u}{\partial t}=G+\frac{\partial^2 u}{\partial y^2}-H^2u-\frac{u}{K_1} \quad (7)$$

$$\mathrm{Pr}\frac{\partial T}{\partial t}=\mu\frac{\partial^2 T}{\partial y^2}+Br\left[\left(\frac{\partial u}{\partial y}\right)^2+H^2u^2\right]+\mathrm{a}\left[(1+\pounds T)^m\left(e^{\frac{T}{1+\pounds T}}+¥e^{\frac{rT}{1+\pounds T}}\right)+\quad T\right] \quad (8)$$

With the corresponding initial and boundary conditions

$$u(y,0)=0,T(y,0)=0,u(0,t)=0,u(1,t)=1,T(0,t)=0,T(1,t)=0 \quad (9)$$

where u, T, G, H, Br, a, $¥$, Pr, r, $\pounds$, K_1 and μ are as defined in the nomenclature.

3.0 Method of Solution

A combined form of the Laplace transform method (LTM) with the differential transform method (DTM) called LDTM will be used to solve equations (7) - (9). The combined method is capable of handling non-homogeneous linear partial differential equations with variable coefficient. The advantage of the proposed method is its capability of combining the two powerful methods for obtaining exact solutions. Marwan et al.[17].

4.0 Differential Transform Method

The differential transformation of the derivative of the function $u(y)$ is defined about a point $y=y_0$ as [18]

$$U(k)=\frac{1}{k!}\left[\frac{d^k}{dy^k}u(y)\right]_{y=y_0} \quad (10)$$

And the differential inverse transform $U(k)$ is defined as

$$u(y)=\sum_{k=0}^{\infty}U(k)(y-y_0)^k \quad (11)$$

Substituting (8) and (9), we obtain

$$u(y)=\sum_{k=0}^{\infty}\frac{1}{k!}\left[\frac{d^k}{dy^k}u(y)\right]_{y=y_0}(y-y_0)^k \quad (12)$$

In this application, y_0 is taken to be zero, (10) becomes

$$u(y)=\sum_{k=0}^{\infty} y^k \frac{1}{k!}\left[\frac{d^k}{dy^k}u(y)\right]_{y=0} \tag{13}$$

Table 1: Fundamental operations of Differential Transform

Original Function	Transformed Function
$u(y)=g(y)\pm h(y)$	$U(k)=G(k)\pm H(k)$
$u(y)=y^n$	$U(k)=¢(k-n)=\begin{cases}1, k=n\\ 0, otherwise\end{cases}$
$u(y)=\frac{du}{dy}$	$U(k)=(k+1)U(k+1)$
$u(y)=\frac{d^2u}{dy^2}$	$U(k)=(k+1)(k+2)U(k+2)$
$u(y)=\frac{d^nu}{dy^n}$	$U(k)=(k+1)(k+2)...U(k+n)$
$u(y)=u(y)v(y)$	$U(k)=\sum_{r=0}^{k}U(r)V(k-r)$
$u(y)=u(y)\frac{dv}{dy}$	$U(k)=\sum_{r=0}^{k}(k-r+1)U(r)V(k-r+1)$
$u(y)=u(y)\frac{d^2v}{dy^2}$	$U(k)=\sum_{r=0}^{k}(k-r+1)(k-r+2)U(r)V(k-r+2)$

5.0 Solution to the Problem

Applying Laplace Transform to equations (7) and (8) with boundary condition (9), we obtain

$$su(y,s)-u(y,0)=\frac{G}{s}+\frac{\partial^2 u}{\partial y^2}-H^2u-\frac{u}{K_1} \tag{14}$$

$$\Pr(sT(y,s)-T(y,0))=\mu\frac{\partial^2\hat{T}}{\partial y^2}+Br\left[\left(\frac{\partial\hat{u}}{\partial y}\right)^2+H^2\hat{u}^2\right]+a\left[(1+£\hat{T})^m\left(e^{\frac{\hat{T}}{1+£\hat{T}}}+¥e^{\frac{r\hat{T}}{1+£\hat{T}}}\right)+\hat{T}\right] \tag{15}$$

$$u(y,0)=0, T(y,0)=0, u(0,s)=0, u(1,s)=\frac{1}{s}, T(0,s)=0, T(1,s)=0 \tag{16}$$

By applying DTM to equations (11) and (12), we respectively have

$$U(k+2)=\frac{k!}{(k+2)!}\left[sU(k)-\frac{G}{s}¢(k)+H^2U(k)-\frac{U(k)}{K_1}\right] \tag{17}$$

And

$$T(k+2) := \frac{k!}{\omega\cdot(k+2)!}\left(Pr\cdot s\cdot T(k) - Br\cdot\left(\sum_{l=0}^{k}(l+1)(k-l+1)\cdot U(l+1)\cdot U(k-l+1) + H^2\cdot\sum_{l=0}^{k}U(l)\cdot U(k-l)\right) - \lambda\cdot\left(\delta(k) + (1+m\cdot\varepsilon)\cdot T(k) - \left(\varepsilon - \frac{1}{2} - m\cdot\varepsilon - \frac{m\cdot(m-1)\cdot\varepsilon^2}{2}\right)\cdot\left(\sum_{l=0}^{k}T(l)\cdot T(k-l)\right) + \left(\varepsilon^2 - \varepsilon + \frac{1}{6} - m\cdot\varepsilon^2 + \frac{m\cdot\varepsilon}{2} + \frac{m\cdot(m-1)\cdot\varepsilon^2}{2} + \frac{m\cdot(m-1)\cdot(m-2)\cdot\varepsilon^3}{6}\right)\cdot\left(\sum_{q=0}^{k}\sum_{l=0}^{q}T(l)\cdot T(q-l)\cdot T(k-q)\right) - \left(\varepsilon^3 - \frac{3}{2}\cdot\varepsilon^2 + \frac{1}{2}\cdot\varepsilon - m\cdot\varepsilon^3 + m\cdot\varepsilon^2 - \frac{m\cdot\varepsilon}{6} + \frac{m\cdot(m-1)\cdot\varepsilon^2}{2} - \frac{m\cdot(m-1)\cdot\varepsilon^2}{4} - \frac{m\cdot(m-1)\cdot(m-2)\cdot\varepsilon^3}{6}\right)\cdot\left(\sum_{p=0}^{k}\sum_{q=0}^{p}\sum_{l=0}^{q}T(l)\cdot T(q-l)\cdot T(p-q)\cdot T(k-p)\right) + \gamma\cdot\left(\delta(k) + (r+m\cdot\varepsilon)\cdot T(k) - \left(r\cdot\varepsilon - \frac{r^2}{2} - m\cdot\varepsilon\cdot r - \frac{m\cdot(m-1)\cdot\varepsilon^2}{2}\right)\cdot\left(\sum_{l=0}^{k}T(l)\cdot T(k-l)\right) + \left(r\cdot\varepsilon^2 - r^2\cdot\varepsilon + \frac{r^3}{6} - m\cdot\varepsilon^2\cdot r + \frac{m\cdot\varepsilon\cdot r^2}{2} + \frac{m\cdot(m-1)\cdot\varepsilon^2\cdot r}{2} + \frac{m\cdot(m-1)\cdot(m-2)\cdot\varepsilon^3}{6}\right)\cdot\left(\sum_{q=0}^{k}\sum_{l=0}^{q}T(l)\cdot T(q-l)\cdot T(k-q)\right) - \left(r\cdot\varepsilon^3 - \frac{3\cdot r\cdot\varepsilon^2}{2} + \frac{r^3\cdot\varepsilon}{2} - m\cdot\varepsilon^3\cdot r + m\cdot\varepsilon^2\cdot r^2 - \frac{m\cdot\varepsilon\cdot r^3}{6} + \frac{m\cdot(m-1)\cdot\varepsilon^3\cdot r}{2} - \frac{m\cdot(m-1)\cdot\varepsilon^2\cdot r^2}{4} - \frac{m\cdot(m-1)\cdot(m-2)\cdot\varepsilon^3\cdot r}{6}\right)\cdot\left(\sum_{p=0}^{k}\sum_{q=0}^{p}\sum_{l=0}^{q}T(l)\cdot T(q-l)\cdot T(p-q)\cdot T(k-p)\right) + \beta\cdot T(k)\right)\right)\right) \quad (18)$$

6.0 Skin Friction and Nusselt Number

7.0 Skin friction

The shear stress on the channel boundaries $y = 0$ and $y = 1$ is given by

$$\tau = \frac{\partial u}{\partial y} \quad (19)$$

8.0 Nusselt Number

$$Nu = -\frac{\partial T}{\partial y} \quad (20)$$

9.0 Results and Discussion

The problem of unsteady radiative hydromagnetic internal heat generating fluid flow through a porous channel of a two-step exothermic chemical reaction under different chemical kinetics with isothermal wall temperature is addressed in this study. The velocity profiles against y and t are presented while that of temperature are presented against y only. Solution of the problem is evaluated using numerical data and the results obtained are illustrated through graphs. The Skin friction and the Nusselt numbers are computed and tabulated.

Fig. 2 displays the effects of variations in pressure gradient G on fluid velocity against y . Increase in the pressure gradient results in increase on the fluid velocity i.e. the maximum velocity occurs as the pressure gradient increases which implies that the more the pressure is applied in the channel, the faster the fluid flow. Fig. 3 shows the effects of variations in Hartmann number H on fluid velocity against y .This shows that increase in the parameter H leads to increase in fluid velocity. That is, maximum velocity will occur at the maximum value of H . The fluid velocity profile shown in Fig. 4 indicates that the fluid velocity increases with a gradual increase in the porosity parameter K_1. It is observed in Fig. 5 that as the pressure gradient increases, velocity profile increases with respect to time. Fig. 6 shows the effect of variations in Hartmann number H on fluid velocity. This shows that increase in the parameter H leads to the reduction in fluid velocity. That is, maximum velocity will occur at the minimum value of H . An increase in the fluid velocity is observed with increasing values of the porosity parameter K_1 in Fig.7.

The effects of different chemical kinetics are presented in Fig. 8. It is observed that temperature profile increases as the numerical exponent m increases from -2, 0 to 0.5 (i.e. Sensitized, Arrhenius and Bimolecular chemical kinetics). It can be deduced from Figs. 9a, 9b and 9c that the variation of Hartmann number parameter under different chemical kinetics has no significant changes in the temperature profiles. Figs. 10a, 10b and 10c show the temperature profiles for variation in pressure gradient under different chemical kinetics. Increase in pressure gradient brought about a decrease in the temperature profiles.

The effects of heat source parameter on temperature profiles under different chemical kinetics are presented in Figs. 11a, 11b and 11c. It is cleared from these figures that an increase in the heat source parameter increases the temperature profiles.In the system, Figs. 12a, 12b and 12c display the evolution of temperature field under different chemical kinetics. It is noteworthy that there is general increase in the temperature profile with increasing values of Frank-Kamenetskii parameter a . This is as a result of increase in the rate of internal heat generation activities in the channel and exothermic reaction.The influence of the Prandtl number Pr on the temperature profiles are illustrated in Figs. 13a, 13b and 13c under different chemical kinetics. The numerical results indicates that the influence of increasing values of Pr number causes a decrease in the source term, hence reduce the temperature profiles.

Fig. 14a depicts the effect of activation energy parameter on temperature profile under sensitized kinetics. It is observed that the temperature profiles reduce with an increase in the activation energy parameter.In Fig. 14b, the effect of activation energy parameter on the temperature profiles under Arrhenius kinetics is insignificant.Fig. 14c shows the effect of activation energy parameter on temperature profile under Bimolecular kinetics. It is seen that the temperature profiles increase with an increase in the activation energy parameter.

Figs. 15a, 15b and 15c depict the effects of the two-step exothermic reaction parameter ¥ on temperature profiles under different chemical kinetics. It is noted that increase in two-step exothermic reaction parameter correspond to increase in the temperature profiles.

The influences of activation energy ratio parameter ʳon the temperature profiles under different kinetics are shown in Figs. 16a, 16b and 16c. It is found that increase in the activation energy ratio parameter result in increase in the temperature profiles.

The effects of radiation parameterω on the profiles under different kinetics are presented in Figs. 17a, 17b and 17c. From these figures, it can be seen that the temperature profiles decreased with an increase in the radiation parameter.

Table 2: Skin Friction coefficients for different values of G, H and K_1.

Parameters	y=0	y=1
G=1	0.92678	1.56310
G=3	1.87797	0.49406
G=5	2.82916	-0.57499
K_1 =1	0.92678	1.56310
K_1 =3	0.90689	1.57512
K_1 =5	0.90301	1.57732
H=1	0.92678	1.56310
H=3	0.73433	1.61467
H=5	0.53506	1.64659

Table 3: The Nusselt Number for different values of H,G,Pr,Br, γ,λ,£ ,β,ω and runder Sensitized kinetics(m=-2)

Parameters	y=0	y=1
H=1	-1.60280	3.19160
H=3	-1.60287	3.19425
H=5	-1.60299	3.19741
G=1	-1.60280	3.19160
G=3	-1.58531	3.10435
G=5	-1.55179	2.94691
Pr=0.71	-1.60280	3.19160
Pr=1	-1.23244	2.45088
Pr=3	-0.46790	2.92181
Br=1	-1.60280	3.19160
Br=3	-1.59780	3.15363
Br=5	-1.59780	3.11566
¥ =1	-1.60280	3.19160
¥ =3	-3.85306	7.69212
¥ =5	-6.94286	13.87172
λ= 0.5	-1.60280	3.19160
λ= 1.5	-6.47061	12.92724
λ=2.5	-14.49910	28.98421
£ =0.1	-1.60280	3.19160
£ =0.3	-1.51490	3.01581
£ =0.5	-1.43182	2.84965
ω=1	-1.60280	3.19160
ω=3	-0.68756	1.37045
ω=5	-0.29478	0.58635
r=1	-1.60280	3.19160
r=3	-1.84548	3.67697
r=5	-2.12488	4.23577
β= 0.5	-1.60280	3.19160
β= 1.5	-1.71987	3.42574
β=2.5	-1.84548	3.67697

Table 4: The Nusselt Number for different values of H,G,Pr,Br, γ,λ, £ ,β, ω and runder Arrhenius kinetics(m=0)

Parameters	y=0	y=1
H=1	-1.64864	3.28329
H=3	-1.64871	3.28594
H=5	-1.64883	3.28910
G=1	-1.64864	3.28329
G=3	-1.63100	3.19573
G=5	-1.59718	2.03770
Pr=0.71	-1.64864	3.28329
Pr=1	-1.25736	2.50072
Pr=3	-0.47104	2.92808
Br=1	-1.64864	3.28329
Br=3	-1.64360	3.24523
Br=5	-1.63856	3.20717
¥ =1	-1.64864	3.28329
¥ =3	-4.07647	8.13895
¥ =5	-7.55525	15.09651
λ= 0.5	-1.64864	3.28329
λ= 1.5	-7.04136	14.06873
λ=2.5	-16.69234	33.37069
£ =0.1	-1.64864	3.28329
£ =0.3	-1.64864	3.28329
£ =0.5	-1.64864	3.28329
ω=1	-1.64864	3.28329
ω=3	-0.70724	1.40982
ω=5	-0.30303	0.60325
r=1	-1.64864	3.28329
r=3	-1.89826	3.78252
r=5	-2.18564	4.35729
β= 0.5	-1.64864	3.28329
β= 1.5	-1.76905	3.52412
β=2.5	-1.89826	3.78252

Table 5: The Nusselt Number for different values of H,G,Pr,Br, γ,λ,β, ω and runder Bimolecular chemical kinetics (m=0.5)

Parameters	y=0	y=1
H=1	-1.66030	3.30661
H=3	-1.66038	3.30926
H=5	-1.66049	3.31242
G=1	-1.66030	3.30661
G=3	-1.64263	3.21898
G=5	-1.60873	3.06080
Pr=0.71	-1.66030	3.30661
Pr=1	-1.26367	2.51334
Pr=3	-0.47182	0.92965
Br=1	-1.66030	3.30661
Br=3	-1.65525	3.26853
Br=5	-1.65021	3.23045
γ=1	-1.66030	3.30661
γ=3	-4.13432	8.25464
γ=5	-7.71661	15.41923
λ= 0.5	-1.66030	3.30661
λ= 1.5	-7.19175	14.36950
λ=2.5	-17.29065	34.56730
£ =0.1	-1.66030	3.30661
£ =0.3	-1.68388	3.35376
£ =0.5	-1.70779	3.40158
ω=1	-1.66030	3.30661
ω=3	-0.71225	1.41983
ω=5	-0.30518	0.60756
r=1	-1.66030	3.30661
r=3	-1.91169	3.80938
r=5	-2.20110	4.38821
β= 0.5	-1.66030	3.30661
β= 1.5	-1.78157	3.54915
β=2.5	-1.96635	3.80938

The expressions for the Skin friction and Nusselt number are given in equations (20) and (21) respectively. The results are tabulated in Table 2, Table 3, Table 4 and Table 5 for various values of fluid parameters under different chemical kinetics. In order to ascertain the contributions of each parameter, we varied one parameter and taken the rest as default fixed values. It is observed from Table 2 that an increase in the parameter G created a significant rise in the skin friction while increase in parameters H and K_1 resulted in reduction in the skin friction coefficient at the wall $y = 0$. It can be noted that an increase in the parameter G causes a reduction in the skin friction while increase in the parameters H and K_1 produced a rise in the skin friction at the wall $y = 1$.

For the Nusselt number under Sensitized chemical kinetics (i.e. $m = -2$) in Table 3, increase in H, ¥, ª, r and resulted in decrease in the Nusselt number while increase in G, Pr, Br, £ and ¥ caused increase in the Nusselt number at the wall $y = 0$. At the wall $y = 1$, it is observed that increase in H, ¥, ª, r and correspondingly increase the Nusselt number while the reverse is the case for increasing values of G, Pr, Br, £ and µ.

Nusselt number under Arrhenius chemical kinetics (i.e. $m = 0$) is shown in Table 4. It is noted that increase in the parameters H, ¥, ª, and r retard the Nusselt number while increase H, G, Pr, Br and µ increase the Nusselt number at the wall $y = 0$. No effect was observed on the Nusselt number at the wall $y = 0$ and $y = 1$ when the parameter £ was increased. Increase in the parameters H, ª, and r resulted in increase in the Nusselt number while increase in G, Pr, Br and µ causes reduction in the Nusselt number at the wall $y = 1$. As for the Nusselt number under

Bimolecular chemical kinetics (i.e. $m = 0.5$) in Table 5, we observed that an increase in H, ¥, ª, £, and r reduces the Nusselt number while an increase in the parameters G, Pr, Br and μ increases the Nusselt number at the wall $y = 0$. Increasing the values of H, ¥, ª, £, and r brought about a corresponding increase in the Nusselt number while increase in G, Pr, Br and μ reduce the Nusselt number at the wall $y = 1$.

10.0 Conclusion

The influences of radiation and heat transfer on unsteady reactive hydromagnetic internal heat generating fluid flow through a porous channel with two-step exothermic chemical reaction have been investigated. The governing equations from the formulation of the problem are non-dimensionalised and solved using a combined Laplace Differential Transform Method (LDTM) to obtain the velocity and temperature distributions. Computed results are presented graphically to study their dependence on the important controlling physical parameters. It is observed that:

(i) An increase in pressure gradient G, magnetic field parameter H and porosity parameter K_1 against y cause a rise in the velocity profile. Similarly, an increase in pressure gradient, magnetic field and porosity parameter against t cause a rise in the velocity profile for G and K_1 but reduction for H.

(ii) An increase in chemical kinetics m, activation energy ratio parameter r, two-step exothermic reaction parameter ¥, activation energy parameter £ (under Bimolecular kinetics), heat source parameter , Frank-Kamenestkii parameter ª leads to increase in the temperature profiles.

(iii) An increase in radiation parameter μ, Prandtl number Pr and activation energy parameter £ (under Sensitized kinetics) has a retarding effect on the temperature profile.

(iv) An increase in magnetic field H and activation energy parameter £ (under Arrhenius kinetics) has no significant effects.

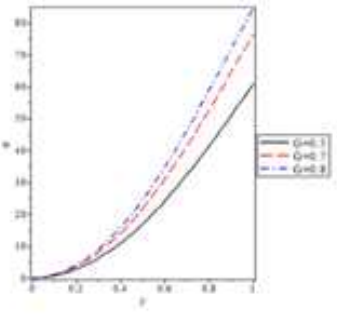

Fig 2: Velocity profiles for different values of G

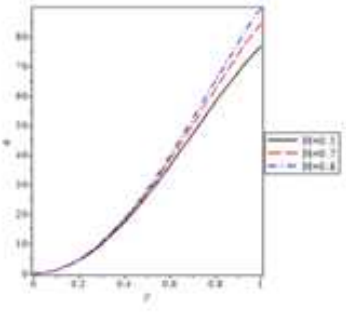

Fig 3 : Velocity profiles for different values of H

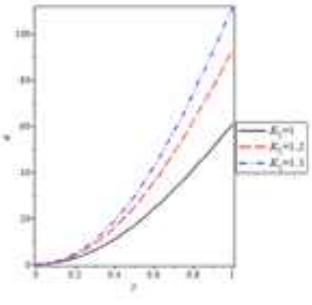

Fig 4: Velocity profiles for different values of K

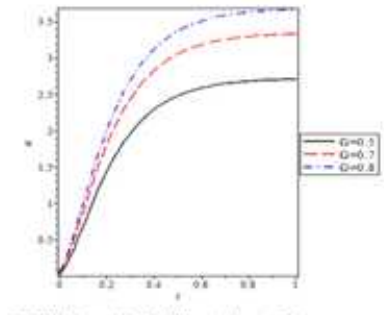

Fig 5: Velocity profiles for different values of G

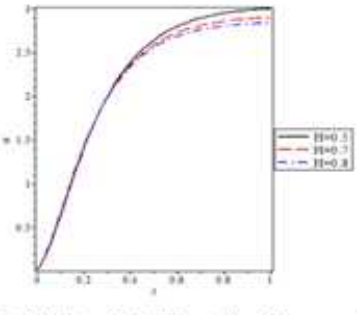

Fig 6: Velocity profiles for different values of H

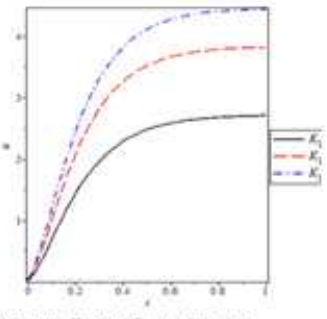

Fig 7: Velocity profiles for different values of K

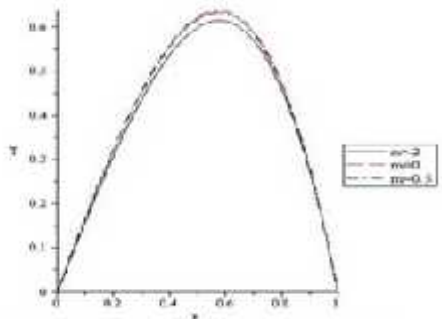

Fig 8: Temperature Profiles for different kinetics

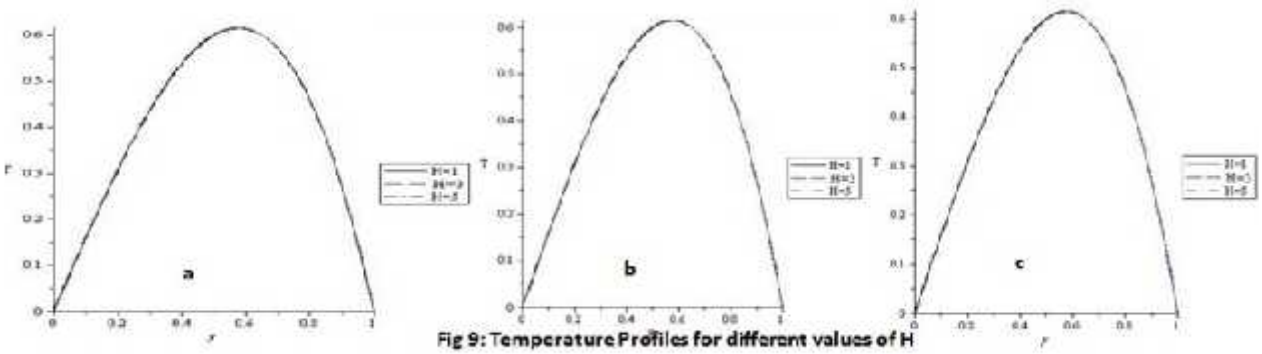

Fig 9: Temperature Profiles for different values of H

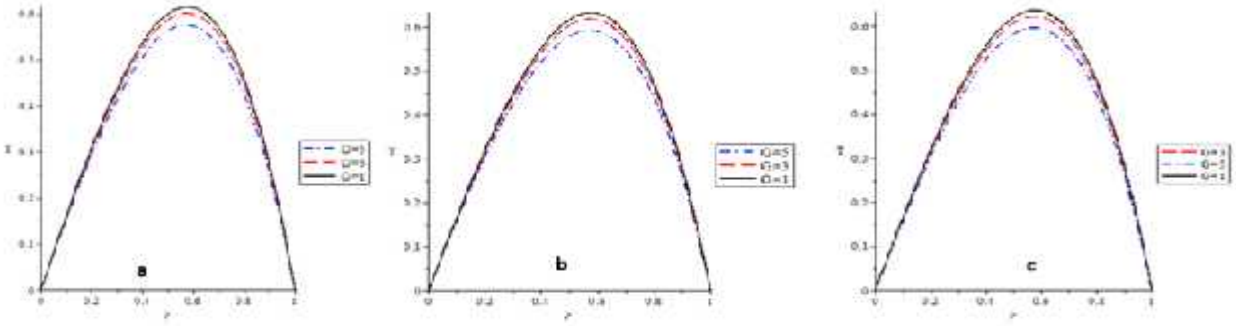

Fig 10: Temperature profiles for different values of G

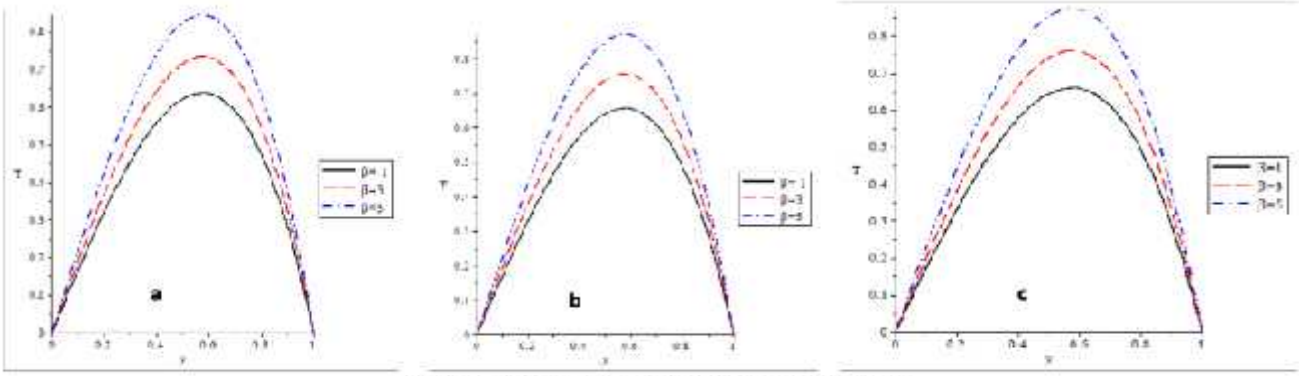

Fig 11: Temperature profiles for different values of β

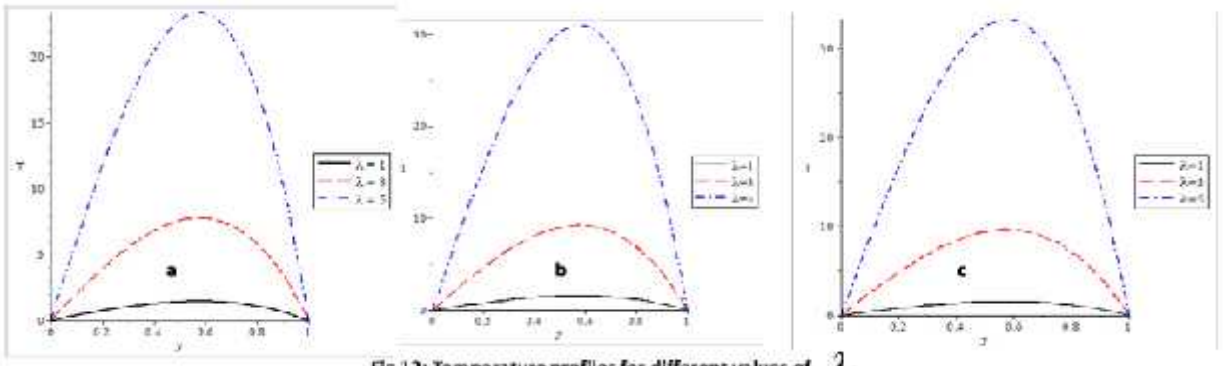

Fig 12: Temperature profiles for different values of λ

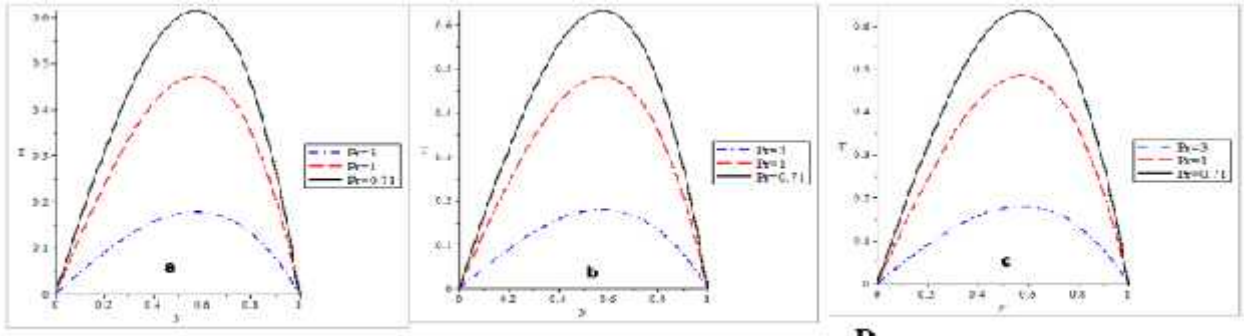

Fig 13: Temperature profiles for different values of $\mathbf{Pr}$

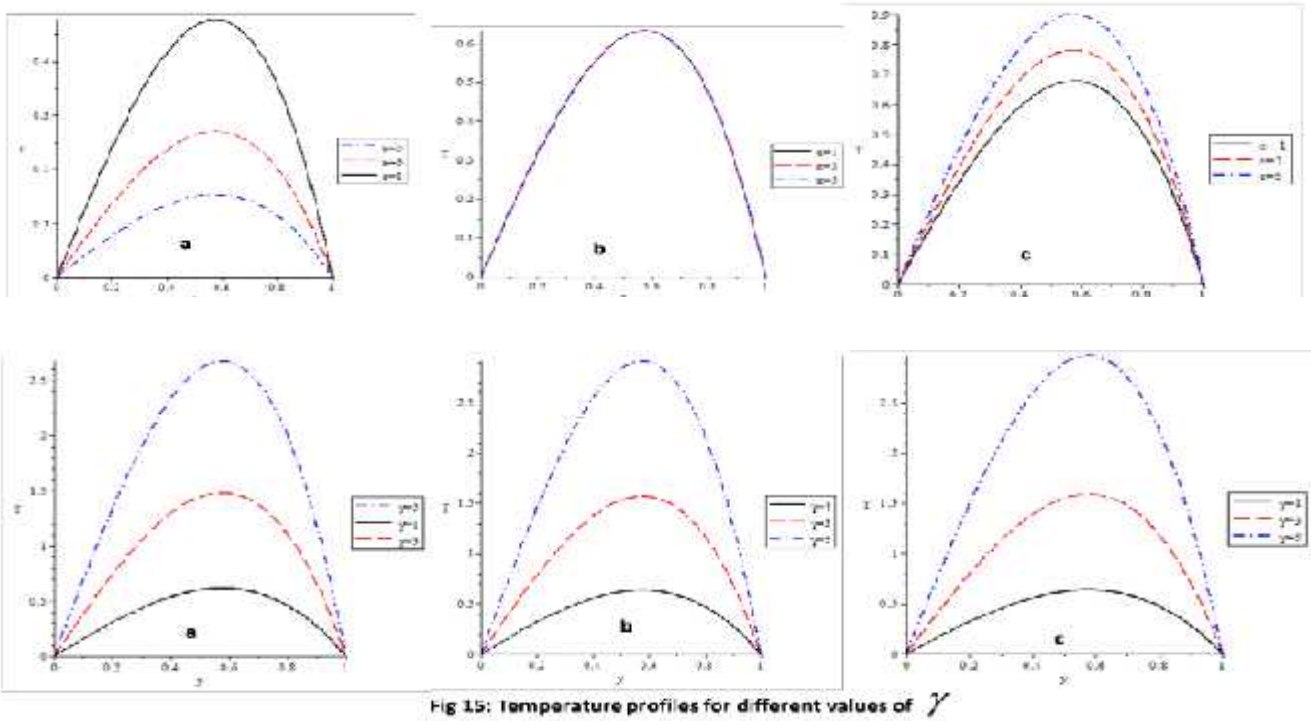

Fig 15: Temperature profiles for different values of γ

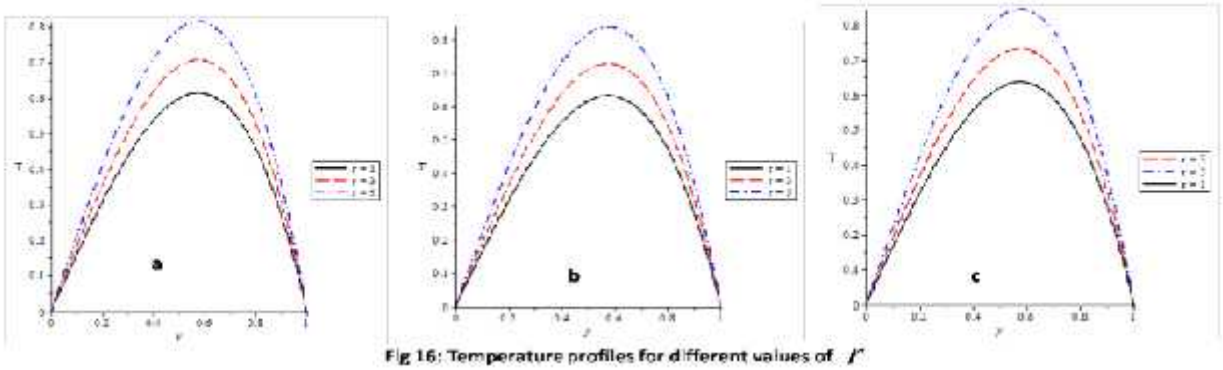

Fig 16: Temperature profiles for different values of γ

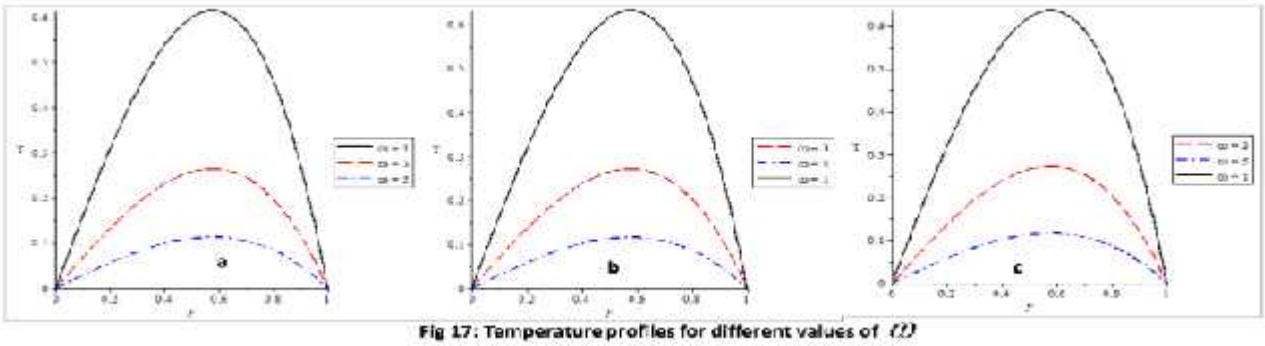

Fig 17: Temperature profiles for different values of Ω

References

[1] Makinde, O. D. (2004). Exothermic explosions in a slab: A case study of series summation technique. International and Mass Transfer, 31(8), 1227-1231.

[2] Balakrishnan, E., Swift, A. \& Wake, G. C. (1996). Critical values for some Non-class A geometries in thermal ignition theory. Math. Comput. Modell. 24, l-10.

[3] Bebernes, J. & Eberly, D. (1989). Mathematical problems from combustion theory. Springer-Verlag, New York.

[4] Frank-Kamenettskii D. A. (1969). Diffusion and heat transfer in chemical kinetics, plenum press, New York.

[5] Makinde, O. D. (2009). Thermal stability of a reactive viscous flow through a porous-saturated channel with convective boundary conditions. Applied Thermal Engineering, 29,1773-1777.

[6] Makinde, O. D. & Anwar Beg, O. (2010). On inherent irreversibility in a reactive hydromagnetic channel flow. Journal of Thermal Science, 19(1), 72-79.

[7] Hassan, A. R. (2014). The Analysis of a Reactive Magnetohydrodynamic Generalized Poiseuille Fluid Flow through a Channel. Unpublished Ph. D Thesis, University of Ilorin.

[8] Makinde, O. D., Olanrewaju, P. O., Titiloye, E. O. & Ogunsola A.W. (2013). On thermal stability of a two-step exothermic chemical reaction in a slab . Journal of Mathematical sciences, 1-15.

[9] Chauhan, D. S. & Rastogi, P. (2010). Radiation Effects on Natural Convection MHD Flow in a Rotating Vertical Porous Channel Partially Filled with a Porous Medium, Applied Mathematical Sciences, 4(13), 643 - 655.

[10] Uwanta, I. J., Sani, M. & Ibrahim, M. O. (2011). MHD Convection Slip Fluid Flow with Radiation and Heat Depositor in a Channel in a Porous Medium. International Journal of Computer Applications, 36(2), 0975-8887.

[11] Hayat T., Awais M., Alsaedi A. & Safdar A. (2014). On Computations for Thermal Radiation in MHD Channel Flow with Heat and Mass Transfer. Plos one, 9(1), 1-5.

[12] Pal D. & Talukdar B. (2013). Influence of Hall Current and Thermal Radiation on MHD Convective Heat and Mass Transfer in a Rotating Porous Channel with Chemical Reaction. International Journal of Engineering Mathematics, 1-13.

[13] Reddy B.P. (2010). Radiation and Viscous Dissipation Effects on Unsteady MHD Free Convective Mass Transfer Flow Past an Infinite Vertical Porous Plate with Hall Current in the Presence of Chemical Reaction. Journal of Engineering Computers & Applied Sciences, 3(4), 5-26.

[14] Bakr, A. A. (2014). Chemically reacting unsteady magnetohydrodynamic oscillatory Slip flow of a micropolar fluid in a planer channel with varying concentration. American Journal of Applied Mathematics, 2(4),141-148.

[15] Singh, K. D. (2010). Exact Solution of MHD Mixed Convection Periodic Flow in a Rotating Vertical Channel with Heat Radiation. Int. Journal of Applied Mechanics and Engineering, 18(3), 853-869.
[16] Brewster, M.Q. (1992). Thermal Radiative Transfer and Properties. John Wiley and sons Inc. New York, USA.
[17] Marwan A., Kamel A., Mohammed A. & Ameina T. (2012). The Combined Laplace Transform-Differential Transform Method for Solving Linear Non-Homogeneous PDES. J. Math. Comput. Sci., 2(3), 1927-5307.
[18] Zhou, J. K. (1986). Differential Transformation and its Applications for Electrical circuits, Huarjung University Press, Wuhan, China